Mathematical Modelling and Control

http://www.aimspress.com/journal/mmc

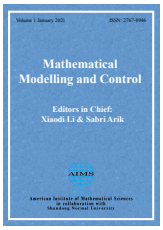

MMC, 6(1): 57–71.
DOI: 10.3934/mmc.2026005
Received: 08 April 2024
Revised: 21 May 2025
Accepted: 09 June 2025
Published: 03 March 2026

Research article

Fractional order dynamics in breast cancer control: a Caputo perspective

Anil Chavada* **and Nimisha Pathak**

Department of Applied Mathematics, Faculty of Technology and Engineering, The Maharaja Sayajirao University of Baroda, Vadodara, Gujarat, India

* **Correspondence:** Email: anilc-appmath@msubaroda.ac.in.

Abstract: In this study, we present a novel fractional-order framework to model the dynamics of breast cancer, incorporating the Liouville–Caputo fractional derivative to capture memory effects inherent in biological systems. The model describes tumor progression and its regulation through chemotherapy within a fractional calculus setting, introducing three control variables-monoclonal antibody drugs, a ketogenic diet, and z-control to influence system behavior. The existence and uniqueness of solutions are rigorously established via Sadovskii's fixed-point theorem, while global stability is examined using Hyers–Ulam stability criteria. Numerical validation is carried out using a predictor–corrector method, and graphical simulations demonstrate the improved accuracy and realism of the fractional-order model compared to its integer-order counterpart. This framework offers a robust theoretical basis for improving breast cancer treatment strategies and has the potential to inform future clinical decision making.

Keywords: breast cancer dynamics; chemotherapy treatment; monoclonal antibody drug; Keto diet; z-control

1. Introduction

Breast cancer is the most well-known and serious illness affecting women worldwide. It is a condition that damages mammary gland cells, leading to the uncontrolled growth of abnormal cells, which can become cancerous within breast tissue [1]. Three critical risk factors for breast cancer are hormonal imbalances, family history, and environmental factors, such as alcohol consumption, poor nutrition, pollutants, and smoking. Treatment options include chemotherapy, hyperthermia, radiation, hormone therapy, surgery, targeted therapies, and the ketogenic diet, all aimed at inhibiting tumor growth [2]. However, each treatment has its own set of side effects, including nausea, fatigue, hair loss, and vertigo. These side effects arise because chemotherapy cannot distinguish between healthy and cancerous tissues, leading to the destruction of both.

Mathematical models have been developed to study the relationship between malignant cells and immune responses during treatment, primarily using integer-order differential equations. Bota et al. [3] present a detailed analysis of mathematical models for breast and ovarian cancers, highlighting the key mechanisms underlying tumor growth. Dey [4] explores mathematical modeling specifically applied to breast cancer treatment, offering important perspectives on treatment efficacy. In addition, Oke [5] investigates optimal control strategies in breast cancer models, to optimize therapeutic outcomes. Shah [6] proposes an adaptive neuro-fuzzy inference system (ANFIS)-based classifier for the diagnosis of breast cancer. In [7], the authors provide the ultimate kernel machine for the diagnosis of breast cancer. The authors in [8] focus on the identification of breast tumors using a hybrid approach combining independent component analysis and deep neural networks. Furthermore, the study [9] discusses the use of a regularized deep neural network for the identification of breast cancer. Wei et al. [10] developed a mathematical model of estrogen receptor (ER) positive breast cancer treatment that incorporates AZD9496 and palbociclib drugs, providing valuable information on the effects of combination

therapy.

One of the fastest-growing fields in mathematical analysis, fractional calculus, studies derivatives and integrals of arbitrary order [11]. Recent advances in fractional calculus suggest that fractional-order models often yield more accurate, useful, and reliable results than traditional integer-order differential equations. Modern fractional derivative operators are increasingly applied to real-world problems in biology, mathematics, physics, engineering, economics, and other scientific and technical fields [12, 13] and references cited therein.

Due to the unique nature of fractional derivatives, where even minor adjustments to the order can lead to significant changes in outcomes, converting models governed by ordinary differential equations (ODEs) into fractional-order differential equations (FDEs) requires precision. Certain phenomena that cannot be adequately represented by integer-order differential equations (IDEs) may be effectively modeled using FDEs. FDEs are especially suitable for biological models due to their relevance to memory and hereditary traits.

The Liouville-Caputo derivative is widely used in modeling because it effectively captures memory and hereditary properties in dynamic systems, which are essential in biological processes. Unlike standard derivatives, it accounts for the influence of past states on current behavior, making it ideal for systems like breast cancer progression, where previous cell interactions and treatments impact ongoing dynamics. Additionally, the Liouville-Caputo derivative allows initial conditions to be set in familiar, integer-order terms, making it compatible with clinical data and enhancing model realism. This approach provides a more accurate and nuanced representation of cancer cell growth, treatment responses, and immune system interactions over time.

The referenced studies underscore the broad utility of the Liouville-Caputo fractional derivative in modeling complex interactions across diverse domains, from epidemiology and environmental science to biological control and disease dynamics. In [14], the author discussed dynamics and numerical analysis of a fractional-order toxoplasmosis model incorporating human and cat populations. In [15], fractional calculus is applied to a COVID-19 model to gain deeper insights into epidemic spread, while [16] discusses the design of a sliding mode controller for fractional chaotic systems, showcasing the robustness benefits in control theory. The authors in [17] provides a robust quasilinearization method combined with generalized shifted Chebyshev functions of the third kind (QLM-SCFTK) matrix approach applied to a biological population model of fractional order considering the carrying capacity. The authors in [18] use a 4D fractional model to address climate complexity through hyperchaotic dynamics, and [19] applies fractional modeling to understand ocean pH dynamics, capturing intricate impacts on marine ecosystems. Extending to ecological systems, [20] explores a three-species food chain model through optimal control strategies, revealing valuable insights for ecological stability. Singh et al. [21] presents a fractional calculus approach to pancreatic cancer therapy by modeling tumor and immune interactions with siRNA treatment.

The authors in [22] presented a note on Lyapunov-type inequalities for fractional boundary value problems with Sturm–Liouville boundary conditions. The authors in [23] performed a qualitative analysis of a Caputo fractional mathematical model of pancreatic cancer. In medical contexts, the authors [24] examine the fractional dynamics of biological pest control in tea plants using the Beddington–DeAngelis response, illustrating its relevance in agricultural systems. In [25], a fractional approach models atmospheric CO_2 dynamics, aiding in understanding greenhouse gas behavior, while [26] utilizes fractional calculus to analyze chemical reactions linked to pattern formation. Additionally, [27] provides a fractional-order model for a childhood disease epidemic, enhancing the analysis of disease control, and [28] uses fractional methods to investigate the Swift–Hohenberg equation, advancing computational techniques in pattern formation. Collectively, these works highlight fractional calculus as a powerful tool for deepening our understanding of complex biological, ecological, environmental, and chemical systems.

Solis et al. [29] proposed a fractional mathematical model of breast cancer that captures the complex population dynamics among cancer stem cells, tumor cells, and healthy cells. Their model also incorporates the effects of excess estrogen and the natural immune response of the body on

these cell populations, providing a more comprehensive framework for understanding tumor progression. Yousef et al. [30] examined the role of mathematical simulations in breast carcinoma treatment, focusing on immuno-chemotherapeutic approaches under controlled conditions involving immune boosters, a ketogenic diet, and the anticancer drug tamoxifen, excluding z-control. In [31], the authors demonstrate the competition between dead and healthy cells under chemotherapy combined with monoclonal antibody therapies and a ketogenic diet. This competition is modeled through a system of nonlinear ordinary differential equations, both with and without z-control. In addition, the study discusses the existence, uniqueness, and stability of equilibrium points. Monoclonal antibodies are conjugated with chemotherapeutic agents to selectively target cancer cells, minimizing damage to healthy tissues.

In the current research, we extend the mathematical model of breast tumor dynamics presented in [31] by incorporating the Liouville-Caputo fractional derivative with a power kernel. This fractional model provides an approximate solution via a numerical approach and includes a qualitative analysis of system behavior.

The organization of this study is as follows: Section 1 outlines the foundational concepts in fractional calculus. Section 2 develops the mathematical model of breast cancer dynamics using a Liouville-Caputo fractional derivative of variable order. Sections 3 and 4 focus on the determination of equilibrium points and the qualitative analysis of the fractional-order model within the Liouville-Caputo framework. Section 5 presents a numerical scheme designed to solve the resulting system of fractional differential equations (FDEs). Numerical results and simulation outcomes are discussed in Section 6 and finally, Section 7 concludes the study with a summary of key findings and future directions.

2. Preliminaries of fractional calculus

Here, we provide some essential definitions used in this paper.

Definition 2.1. *For* $\mathfrak{z} > 0$ *and* $\varphi : \mathbb{R}^+ \to \mathbb{R}$, *the Riemann–Liouville fractional integral operator [11] is defined by*

$$ {}_0I_t^{\mathfrak{z}}(\varphi(t)) = \frac{1}{\Gamma(\mathfrak{z})} \int_0^t (t-\Re)^{\mathfrak{z}-1} \varphi(\Re)\, d\Re, \quad t > 0. \tag{2.1} $$

Definition 2.2. *The Liouville–Caputo fractional derivative [32] of order* $\mathfrak{z} > 0$ *for a function* $\varphi(t)$, *where* $\varphi \in C^{\mathfrak{m}}([0,T])$, *is defined as*

$$ {}_0^{LC}D_t^{\mathfrak{z}}(\varphi(t)) = \frac{1}{\Gamma(\mathfrak{m}-\mathfrak{z})} \int_0^t (t-\Re)^{\mathfrak{m}-\mathfrak{z}-1} \varphi^{(\mathfrak{m})}(\Re)\, d\Re, \quad t > 0, \tag{2.2} $$

where $\mathfrak{m}-1 < \mathfrak{z} \leq \mathfrak{m}$, *and* $\mathfrak{m} \in \mathbb{N}$.

3. Mathematical modelling of breast cancer dynamics

In this section, we consider modified breast cancer epidemiology with control parameters [31]. We replace conventional derivatives by the Liouville-Caputo derivative as shown in (2.2) to obtain the fractional order system. The fractionalization approach addresses dimensional disparity in time-based fractional-order differential equations by increasing the biological parameters on the right side to fractional powers matching those on the left.

A system of fractional differential equations (FDEs) is formulated in the following manner:

$$ \begin{aligned} {}_0^{LC}D_t^{\mathfrak{z}}H(t) &= J_1(t,H,D,A); \quad H(0) = H_0, \\ {}_0^{LC}D_t^{\mathfrak{z}}D(t) &= J_2(t,H,D,A); \quad D(0) = D_0, \\ {}_0^{LC}D_t^{\mathfrak{z}}A(t) &= J_3(t,H,D,A); \quad A(0) = A_0, \end{aligned} \tag{3.1} $$

where

$$ \begin{aligned} J_1(t,H,D,A) &= l_H - d_1 HD - \Delta_H, \\ J_2(t,H,D,A) &= l_D - d_2 HD - \Delta_D - uD, \\ J_3(t,H,D,A) &= i_g - h_w A - \omega_1 - \omega_2 - u_1(t)A. \end{aligned} $$

Table 1 provides a description of the parameters and their values. All parameters inside the model are considered to be positive constants with the following definitions:

- $H(t)$: healthy (normal) cells population.
- $D(t)$: dead (cancer) cells.
- $A(t)$: monoclonal antibody drugs.
- $l_H = a_1 H\left(1 - \frac{H}{b_1}\right)$: represents logarithmic growth of healthy cells with growth rate a_1 and carrying capacity b_1.

- d_1HD: competition between cancer cells and healthy cells at a rate d_1.

- $\Delta_H = \frac{e_1HA}{f_1+H}$: holling class-II term indicating absorption of normal cells due to chemotherapy and monoclonal antibody medicines at a rate e_1.

- $l_D = a_2D\left(d - \frac{D}{b_2}\right)$: natural growth of cancer cells with growth rate a_2 and carrying capacity b_2; the ketogenic diet impacts cancer cell growth at a steady rate d.

- d_2HD: competition between healthy and cancerous cells at a rate d_2.

- $\Delta_D = \frac{e_2DA}{f_2+D}$: holling type-II term demonstrating absorption of malignant cells due to chemotherapy and monoclonal antibody pharmaceuticals at a rate e_2.

- uD: toxicity of the ketogenic diet causing cancer cell death.

- i_g: rate of infusion of chemotherapy drugs and monoclonal antibody medicines.

- h_wM: rate of elimination of monoclonal antibody pharmaceuticals and chemotherapy agents, with an expulsion rate of h.

- $\omega_1 = \frac{j_1HA}{f_1+H}$: normal cell absorption of monoclonal antibody drugs and chemotherapeutic agents at a rate j_1, expressed as a Holling type-II term.
- f_1: rate without competition, where healthy cell absorption achieves carrying capacity.

- $\omega_2 = \frac{j_2DA}{f_2+D}$: absorption of monoclonal antibody medicines and chemotherapeutic agents by cancer cells at a rate j_2, expressed as a Holling type-II term.
- f_2: rate of absorption where cancer cells acquire carrying capacity in the absence of competition.

- z-control($u_1(t)$): indirect regulation of chemotherapeutic treatment and monoclonal antibody medicines. The expression of $u_1(t)$ is given in [31].

Table 1. Description of the parameters and their values [31].

Parameter	Symbol	Value/Unit
Division rate of Normal cells	a_1	1.5/day
Division rate of Cancer cells	a_2	10.0/day
Transport ability of healthy cells	b_1	1460/day
Transport ability of Cancer cells	b_2	2100/day
Competition rate of malignant cells kills healthy cells	d_1	0.0075 /day
Competition rate of Normal cells kills Cancer cells	d_2	0.005/day
Absorption rate of Normal cells due to combine effect of chemotherapy and monoclonal antibody drugs	e_1	0.000384/day
Absorption rate of Cancer cells due to combine effect of chemotherapy and monoclonal antibody drugs	e_2	0.1216/day
Without competition and absorption normal cells reaches at carrying capacity	f_1	1/day
Without competition and absorption cancer cells reaches at carrying capacity	f_2	1/day
Absorption rate of chemotherapy and monoclonal antibody due to drugs normal cells	j_1	0.001152/day
Absorption rate of chemotherapy and monoclonal antibody due to drugs cancer cells	j_2	0.1152/day
Death rate of cancer cells due to keto diet	u	2.0/day
Infusion rate of chemotherapy and monoclonal antibody drugs	i_g	2450/day
Washout rate of chemotherapy and monoclonal antibody drugs	h_w	9.6/day
Keto diet at a constant pace	d	0.5/day

4. The equilibrium points

There are four equilibrium points of system (3.1). The first is a tumor-free equilibrium point (B_{TFEP}), two are dead equilibrium points (B_{DEP_1} and B_{DEP_2}), and one is the cancerous endemic equilibrium point ($B_{CEEP}(H^*, D^*, A^*)$), which are listed below.

(1) $B_{TFEP}(H^*, 0, A^*)$: This point denotes the absence of cancerous cells and the presence of H^* healthy cells and A^* therapy agent:

$$B_{TFEP}(H^*, 0, A^*) = \left(\frac{\Delta_H}{l_H}, 0, \frac{i_g - \omega_1 - \omega_2}{h_w - u_1(t)}\right).$$

(2) $B_{DEP_1}(0, D^*, A^*)$: This equilibrium point indicates that there are no healthy cells, only D^* dead cells and an A^* quantity of therapeutic agents:

$$B_{DEP_1}(0, D^*, A^*) = \left(0, \frac{l_D - \Delta_D}{u}, \frac{i_g - \omega_1 - \omega_2}{h_w}\right).$$

(3) $B_{DEP_2}(0,0,A^*)$: This point reflects the absence of both dead and healthy cells, with only $i_g h_w^{-1}$ representing the quantity of monoclonal antibody medicines and chemotherapeutic agents:

$$B_{DEP_2}(0,0,A^*) = \left(0,0,i_g h_w^{-1})\right).$$

(4) $B_{CEEP}(H^*,D^*,A^*)$: This represents the scenario in which all three elements-healthy cells, dead cells, and therapy agents are present:

$$B_{CEEP}(H^*,D^*,A^*) = \left(\frac{l_H-\Delta_H}{d_1D^*}, \frac{l_D-\Delta_D}{d_2H^*+u}, \frac{i_g-\omega_1-\omega_2}{h_w+u_1^*}\right).$$

Theorem 4.1. *([31]) Let B_{TFEP} be the system's* (3.1) *tumor-free equilibrium position, and if $a_1^{-1} i_g e_1 < h_w f_1$, then B_{TFEP} exists uniquely, and if*

$$h_w f_1 < \frac{i_g e_1}{a_1} < \frac{(h_w f_1 + b_1(h_w + j_1))^2}{4(h_w + j_1)b_1}$$

admits, then two separate equilibria exist of type B_{TFEP}.

Proof. Available in [31]. □

Theorem 4.2. *([31]) Suppose that $a_2 d > d_2 H^* + u + \frac{e_2 A^*}{f_2}$ and $H^* > \frac{b_1}{2}$, then B_{TFEP} is unstable, and if $H^* > \frac{b_1}{2}$ and $a_2 d < d_2 H^* + u + \frac{e_2 A^*}{f_2}$, then it is asymptotically stable.*

Proof. Available in [31]. □

Theorem 4.3. *([31]) Let B_{DEP_1} be the dead equilibrium point of the system* (3.1) *that exists uniquely if $i_g e_2 < h_w f_2(a_2 d - u)$.*
Also, if

$$h_w f_2(a_2 d - u) < i_g e_2 < \frac{(h_w f_2 a_2 - b_2(a_2 d - u)(h_w + j_2))^2}{4a_2(h_w + j_2)b_2}$$

admits, consequently, two distinct equilibria of type B_{DEP_1} exist.

Proof. Available in [31]. □

Theorem 4.4. *([31]) If $D^* > \frac{db_2}{2}$ and $a_1 > d_1 D^* + \frac{e_1 A^*}{f_1}$, then B_{DEP_1} is unstable and asymptotically stable if $D^* > \frac{db_2}{2}$ and $a_1 < d_1 D^* + \frac{e_1 A^*}{f_1}$.*

Proof. Available in [31]. □

Theorem 4.5. *([31]) Let B_{DEP_2} be the system's* (3.1) *dead point of equilibrium that is asymptotically stable if $a_1 < (f_1 h_w)^{-1} e_1 i_g$ and $a_2 d < (f_2 h_w)^{-1} e_2 i_g$ and unstable if $a_1 > (f_1 h_w)^{-1} e_1 i_g$ and $a_2 d > (f_2 h_w)^{-1} e_2 i_g$.*

Proof. Available in [31]. □

5. Qualitative study of a system involving Liouville–Caputo derivative

Consider the initial value problem (IVP) that will be used in the following subsections:

$$\begin{aligned} {}_0^{LC}D_t^{\mathfrak{z}}\Lambda(t) &= \varphi(t,\Lambda(t)), \quad \mathfrak{z} > 0, \\ \Lambda(0) &= \Lambda_0; \quad \Lambda \in \mathbb{R},\ t \in (0,+\infty). \end{aligned} \tag{5.1}$$

5.1. Solution for the system: existence and uniqueness

Using Sadovskii's fixed point theorem [33], we discuss the existence and uniqueness of solutions of (5.1) by considering a Banach space Y, with $t \in [0,\mathsf{T}]$, and $H, D, A \in \mathsf{C}(\mathfrak{G}, Y) \cap L^1_{\text{loc}}(\mathfrak{G}, Y)$, where $\mathsf{T}, \mathfrak{r} > 0$, and

$$\mathfrak{G} = \{(t,K) : t \in [0,\mathsf{T}],\ K \in \mathbb{B}(0,\mathfrak{r})\}.$$

Let $\mathbb{B} \subset Y$, and let $\Phi : \mathbb{B} \to \mathbb{B}$ be a mapping with the condensation property. Then, there exists a fixed point of Φ within the set $\mathbb{B}$.

Now, consider the IVP (5.1) on the domain

$$\mathfrak{G} = \{(t,K) \in \mathbb{R}\times Y : t \in [0,\mathsf{T}],\ K \in \mathbb{B}(0,\mathfrak{r})\},$$

for some $\mathsf{T}, \mathfrak{r} > 0$. Then, there exist constants $\lambda \in (0,\mathfrak{z})$, $\mathfrak{M}_1{}^*, \mathfrak{M}_2{}^*, L, L_1 \in L_{1/\lambda}([0,\mathsf{T}],\mathbb{R}^+)$, and functions $H_1, H_2, D_1, D_2, A_1, A_2 \in \mathbb{C}(\mathbb{R}, Y) \cap L^1_{\text{loc}}(\mathbb{R}, Y)$ such that

$$H = H_1 + H_2, \quad D = D_1 + D_2, \quad A = A_1 + A_2.$$

To apply Sadovskii's fixed point theorem, the nonlinear components of system (3.1) are decomposed into Lipschitz continuous parts and compact operators. Specifically, we define:

$$H_1(t,H,D,A) = l_H - d_1 HD,$$

$$H_2(t,H,D,A) = -\Delta H = -\frac{e_1 HA}{f_1+H},$$
$$D_1(t,H,D,A) = l_D - d_2 HD - uD,$$
$$D_2(t,H,D,A) = -\Delta D = -\frac{e_2 DA}{f_2+D},$$
$$A_1(t,H,D,A) = i_g - hwA - u_1(t)A,$$
$$A_2(t,H,D,A) = -\omega_1 - \omega_2 = -\frac{j_1 HA}{f_1+H} - \frac{j_2 DA}{f_2+D}.$$

In this decomposition,

- H_1, D_1, A_1 represent the **Lipschitz continuous** components, primarily involving linear and bilinear terms;
- H_2, D_2, A_2 represent the **compact nonlinear terms**, particularly those incorporating Holling type-II responses.

This separation meets the necessary conditions for applying Sadovskii's fixed-point theorem, thereby guaranteeing the existence and uniqueness of solutions for the fractional-order system. The following assumptions are satisfied:

Assumption 1. H_1, D_1, and A_1 are bounded and Lipschitz continuous.

Assumption 2. H_2, D_2, and A_2 are compact.

Assumption 3. Let $\mathcal{F}(t,\cdot)$ be a function from $\mathbb{R}^n$ to $\mathbb{R}^m$, defined for all $(t,K),(t,Q) \in \mathbb{R}\times\mathbb{R}^n$. Then, there exists a function $L_1(t) \geq 0$ such that

$$\|\mathcal{F}(t,K)-\mathcal{F}(t,Q)\| \leq L_1(t)\|K-Q\|, \quad \forall (t,K),(t,Q) \in \mathbb{R}\times\mathbb{R}^n.$$

Applying Eq (2.1) to system (3.1), the lemma can be formulated as follows.

Lemma 5.1. *As the model under discussion was derived with a single condition for each equation, the IVP* (5.1) *is identical to the subsequent system of integral equations:*

$$H(t) = H(0) + \frac{1}{\Gamma(\mathfrak{z})}\int_0^t (t-\mathfrak{K})^{\mathfrak{z}-1} H_1(\mathfrak{K}, H(\mathfrak{K}))\, d\mathfrak{K} + \frac{1}{\Gamma(\mathfrak{z})}\int_0^t (t-\mathfrak{K})^{\mathfrak{z}-1} H_2(\mathfrak{K}, H(\mathfrak{K}))\, d\mathfrak{K},$$

$$D(t) = D(0) + \frac{1}{\Gamma(\mathfrak{z})}\int_0^t (t-\mathfrak{K})^{\mathfrak{z}-1} D_1(\mathfrak{K}, D(\mathfrak{K}))\, d\mathfrak{K} + \frac{1}{\Gamma(\mathfrak{z})}\int_0^t (t-\mathfrak{K})^{\mathfrak{z}-1} D_2(\mathfrak{K}, D(\mathfrak{K}))\, d\mathfrak{K},$$

$$A(t) = A(0) + \frac{1}{\Gamma(\mathfrak{z})}\int_0^t (t-\mathfrak{K})^{\mathfrak{z}-1} A_1(\mathfrak{K}, A(\mathfrak{K}))\, d\mathfrak{K} + \frac{1}{\Gamma(\mathfrak{z})}\int_0^t (t-\mathfrak{K})^{\mathfrak{z}-1} A_2(\mathfrak{K}, A(\mathfrak{K}))\, d\mathfrak{K}.$$

After structuring the above claims, it is now simple to explain the existence and uniqueness of solution (3.1), as shown in the following two theorems.

Theorem 5.1. *Under Assumptions 1 and 2, the IVP* (5.1) *has an optimal solution on the interval* $[0,\mathsf{T}]$*, provided that*

$$\gamma = \frac{q\,\|L\|_{1/\lambda}\,\mathsf{T}^{\theta}}{\Gamma(\mathfrak{z})} < 1,$$

where $\theta = \mathfrak{z} - \lambda$*, and*

$$q = \left(\frac{1-\lambda}{\mathfrak{z}-\lambda}\right)^{1-\lambda}.$$

Proof. Choose a constant $\mathfrak{r} > 0$ such that

$$|H_0| + \frac{q}{\Gamma(\mathfrak{z})}\left(\|\mathfrak{M}_1^*\|_{1/\lambda} + \|\mathfrak{M}_2^*\|_{1/\lambda}\right)\mathsf{T}^{\theta} \leq \mathfrak{r}.$$

Let

$$B_{\mathfrak{r}} = \{K : \|K\| \leq \mathfrak{r}\}$$

be the closed ball in $\mathbb{BC}([0,\mathsf{T}],\mathsf{Y})$ with the sup norm $\|\cdot\|$. Using Lemma 5.1, one can show that the operator

$$H : B_{\mathfrak{r}} \to \mathbb{BC}([0,\mathsf{T}],\mathsf{Y}), \quad \mathsf{K} \mapsto \mathsf{H}_1\mathsf{K} + \mathsf{H}_2\mathsf{K},$$

satisfies the following properties:

$$H_1K(t) = H(0) + \frac{1}{\Gamma(\mathfrak{z})}\int_0^t (t-\mathfrak{K})^{\mathfrak{z}-1} H_1(\mathfrak{K}, K(\mathfrak{K}))\, d\mathfrak{K},$$

$$H_2K(t) = \frac{1}{\Gamma(\mathfrak{z})}\int_0^t (t-\mathfrak{K})^{\mathfrak{z}-1} H_2(\mathfrak{K}, K(\mathfrak{K}))\, d\mathfrak{K},$$

as a solution of (3.1). We show in three steps that $H(t)$ is condensing and thus the existence of a definite point for $H(t)$.

Step 1: We must demonstrate $H(B_\mathfrak{r}) \subset B_\mathfrak{r}$. For $K \in B_\mathfrak{r}$, we have

$$\begin{aligned}
|H(t)| &\leq |H_0| + \frac{1}{\Gamma(\mathfrak{z})}\int_0^t (t-\mathfrak{K})^{\mathfrak{z}-1}\,|H(\mathfrak{K},K(\mathfrak{K}))|\,d\mathfrak{K}\\
&\leq |H_0| + \frac{1}{\Gamma(\mathfrak{z})}\left(\int_0^t (t-\mathfrak{K})^{\mathfrak{z}-1}\,|H_1(\mathfrak{K},K(\mathfrak{K}))|\,d\mathfrak{K}\right.\\
&\quad\left.+\int_0^t (t-\mathfrak{K})^{\mathfrak{z}-1}\,|H_2(\mathfrak{K},K(\mathfrak{K}))|\,d\mathfrak{K}\right)\\
&\leq |H_0| + \frac{1}{\Gamma(\mathfrak{z})}\int_0^t (t-\mathfrak{K})^{\mathfrak{z}-1}\mathfrak{M}_1{}^*(\mathfrak{K})\,d\mathfrak{K}\\
&\quad+\frac{1}{\Gamma(\mathfrak{z})}\int_0^t (t-\mathfrak{K})^{\mathfrak{z}-1}\mathfrak{M}_2{}^*(\mathfrak{K})\,d\mathfrak{K}\\
&\leq |H_0| + \frac{1}{\Gamma(\mathfrak{z})}\left(\int_0^t (t-\mathfrak{K})^{\frac{\mathfrak{z}-1}{1-\lambda}}d\mathfrak{K}\right)^{1-\lambda}\left(\int_0^t (\mathfrak{M}_1{}^*(\mathfrak{K}))^{\frac{1}{\lambda}}d\mathfrak{K}\right)^{\lambda}\\
&\quad+\frac{1}{\Gamma(\mathfrak{z})}\left(\int_0^t (t-\mathfrak{K})^{\frac{\mathfrak{z}-1}{1-\lambda}}d\mathfrak{K}\right)^{1-\lambda}\left(\int_0^t (\mathfrak{M}_2{}^*(\mathfrak{K}))^{\frac{1}{\lambda}}d\mathfrak{K}\right)^{\lambda}\\
&\leq |H_0| + \frac{q\left(\|\mathfrak{M}_1{}^*\|_{\frac{1}{\lambda}} + \|\mathfrak{M}_2{}^*\|_{\frac{1}{\lambda}}\right)}{\Gamma(\mathfrak{z})}\mathsf{T}^{\theta} \leq \mathfrak{r},
\end{aligned}$$

and thus $H(B_\mathfrak{r}) \subset B_\mathfrak{r}$.

Step 2: We illustrate that H_1 is a contraction. Let $K, Q \in B_\mathfrak{r}$. Then,

$$\begin{aligned}
&|H_1(K(t)) - H_1(Q(t))|\\
&\leq \frac{1}{\Gamma(\mathfrak{z})}\int_0^t (t-\mathfrak{K})^{\mathfrak{z}-1}L(\mathfrak{K})\,|K(\mathfrak{K})-Q(\mathfrak{K})|\,d\mathfrak{K}\\
&\leq \frac{1}{\Gamma(\mathfrak{z})}\left(\int_0^t (t-\mathfrak{K})^{\frac{\mathfrak{z}-1}{1-\lambda}}d\mathfrak{K}\right)^{1-\lambda}\left(\int_0^t L^{\frac{1}{\lambda}}(\mathfrak{K})\,d\mathfrak{K}\right)^{\lambda}\|K-Q\|\\
&\leq \frac{q\|L\|_{\frac{1}{\lambda}}\mathsf{T}^{\theta}}{\Gamma(\mathfrak{z})}\|K-Q\|,
\end{aligned}$$

and hence $H_1(t)$ is a contraction with $\|H_1(K) - H_1(Q)\| \leq \gamma\|K-Q\|$.

Step 3: H_2 is compact. For $0 \leq \tau_1 \leq \tau_2 \leq \mathsf{T}$, we have

$$\begin{aligned}
&|H_2(K(\tau_2)) - H_2(K(\tau_1))|\\
&\leq \frac{1}{\Gamma(\mathfrak{z})}\left|\int_0^{\tau_2}(\tau_2-\mathfrak{K})^{\mathfrak{z}-1}H_2(\mathfrak{K},K(\mathfrak{K}))\,d\mathfrak{K}\right|\\
&\quad-\frac{1}{\Gamma(\mathfrak{z})}\left|\int_0^{\tau_1}(\tau_1-\mathfrak{K})^{\mathfrak{z}-1}H_2(\mathfrak{K},K(\mathfrak{K}))\,d\mathfrak{K}\right|\\
&\leq \frac{1}{\Gamma(\mathfrak{z})}\left|\int_0^{\tau_1}(\tau_2-\mathfrak{K})^{\mathfrak{z}-1}H_2(\mathfrak{K},K(\mathfrak{K}))\,d\mathfrak{K}\right|\\
&\quad+\frac{1}{\Gamma(\mathfrak{z})}\left|\int_{\tau_1}^{\tau_2}(\tau_2-\mathfrak{K})^{\mathfrak{z}-1}H_2(\mathfrak{K},K(\mathfrak{K}))\,d\mathfrak{K}\right|\\
&\quad-\frac{1}{\Gamma(\mathfrak{z})}\left|\int_0^{\tau_1}(\tau_1-\mathfrak{K})^{\mathfrak{z}-1}H_2(\mathfrak{K},K(\mathfrak{K}))\,d\mathfrak{K}\right|\\
&\leq \frac{1}{\Gamma(\mathfrak{z})}\int_0^{\tau_1}\left((\tau_1-\mathfrak{K})^{\mathfrak{z}-1}-(\tau_2-\mathfrak{K})^{\mathfrak{z}-1}\right)|H_2(\mathfrak{K},K(\mathfrak{K}))|\,d\mathfrak{K}\\
&\quad+\frac{1}{\Gamma(\mathfrak{z})}\int_{\tau_1}^{\tau_2}(\tau_2-\mathfrak{K})^{\mathfrak{z}-1}\,|H_2(\mathfrak{K},K(\mathfrak{K}))|d\mathfrak{K}\\
&\leq \frac{1}{\Gamma(\mathfrak{z})}\int_0^{\tau_1}\left((\tau_1-\mathfrak{K})^{\mathfrak{z}-1}-(\tau_2-\mathfrak{K})^{\mathfrak{z}-1}\right)\mathfrak{M}_y{}^*(\mathfrak{K})d\mathfrak{K}\\
&\quad+\frac{1}{\Gamma(\mathfrak{z})}\int_{\tau_1}^{\tau_2}(\tau_2-\mathfrak{K})^{\mathfrak{z}-1}\mathfrak{M}_y{}^*(\mathfrak{K})d\mathfrak{K}\\
&\leq \frac{1}{\Gamma(\mathfrak{z})}\left(\int_0^{\tau_1}\left((\tau_1-\mathfrak{K})^{\frac{\mathfrak{z}-1}{1-\lambda}}-(\tau_2-\mathfrak{K})^{\frac{\mathfrak{z}-1}{1-\lambda}}\right)d\mathfrak{K}\right)^{1-\lambda}\\
&\quad\times\left(\int_0^{\tau_1}\left(\mathfrak{M}_y{}^*(\mathfrak{K})\right)^{\frac{1}{\lambda}}d\mathfrak{K}\right)^{\lambda}+\frac{1}{\Gamma(\mathfrak{z})}\left(\int_{\tau_1}^{\tau_2}(\tau_2-\mathfrak{K})^{\frac{\mathfrak{z}-1}{1-\lambda}}d\mathfrak{K}\right)^{1-\lambda}\\
&\quad\times\left(\int_0^{\tau_1}\left(\mathfrak{M}_y{}^*(\mathfrak{K})\right)^{\frac{1}{\lambda}}d\mathfrak{K}\right)^{\lambda}\\
&\leq \frac{q}{\Gamma(\mathfrak{z})}\left\|\mathfrak{M}_y{}^*\right\|_{\frac{1}{\lambda}}\left[\left((\tau_2-\tau_1)^{\frac{\mathfrak{z}-1}{1-\lambda}}\right)^{1-\lambda}+(\tau_2-\tau_1)^{\mathfrak{z}-\lambda}\right]\\
&\leq \frac{2q\|\mathfrak{M}_2{}^*\|_{\frac{1}{\lambda}}}{\Gamma(\mathfrak{z})}(\tau_2-\tau_1)^{\mathfrak{z}-\lambda}.
\end{aligned}$$

The right side of the inequality is unaffected by K. We establish the compactness of H_2 by its relative compactness in $H_2(B_\mathfrak{r})$ using the Arzela-Ascoli theorem. Due to the fact that H_1 and H_2 have distinct features (contraction and

compactness, respectively), their composite, represented as H, forms a condensing map on $B_{\mathfrak{r}}$. This, along with Lemma 5.1, ensures a definite point for H, which is relevant to the remaining variables, such as $D(t)$ and $A(t)$. □

Theorem 5.2. *Under Assumption 3 and* $\gamma = \frac{q\|L_1\|_{1/\lambda}(\mathsf{T})^{\theta}}{\Gamma(\mathfrak{z})} < 1$, *then a unique solution exists for the IVP* (5.1) *in* $[0, \mathsf{T}]$.

Proof. Define the relation F by

$$FH(t) = H(0) + \frac{1}{\Gamma(\mathfrak{z})}\int_0^t (t-\Re)^{\mathfrak{z}-1} H(\Re, H(\Re))\, d\Re.$$

For $H(t), H_1(t) \in B_{\mathfrak{r}}$, we have

$$\begin{aligned}
&|FH(t) - FH_1(t)| \\
\leq &\frac{1}{\Gamma(\mathfrak{z})}\int_0^t (t-\Re)^{\mathfrak{z}-1} L_1(\Re)\,|H(\Re) - H_1(\Re)|\, d\Re \\
\leq &\frac{1}{\Gamma(\mathfrak{z})}\left(\int_0^t (t-\Re)^{\frac{\mathfrak{z}-1}{1-\lambda}} d\Re\right)^{1-\lambda}\left(\int_0^t L_1{}^{\frac{1}{\lambda}}(\Re)\, d\Re\right)^{\lambda} \|H - H_1\| \\
\leq &\frac{q\|L_1\|_{1/\lambda}(\mathsf{T})^{\theta}}{\Gamma(\mathfrak{z})}\,\|H - H_1\| = \gamma\,\|H - H_1\|.
\end{aligned}$$

Thus, the condition $\gamma = \frac{q\|L_1\|_{1/\lambda}(\mathsf{T})^{\theta}}{\Gamma(\mathfrak{z})} < 1$ ensures the existence of a unique solution. Similarly, a unique solution exists for other model equations. □

5.2. Ulam stability results

We now examine Ulam stability for IVP (5.1). Take $\epsilon > 0$ and a continuous $\varphi : [0, +\infty) \to \mathbb{R}^+$. Consider

$$\left|{}_0^{LC}D_t^{\mathfrak{z}}\Lambda(t) - \varphi(t, \Lambda(t))\right| \leq \epsilon, \tag{5.2}$$

$$\left|{}_0^{LC}D_t^{\mathfrak{z}}\Lambda(t) - \varphi(t, \Lambda(t))\right| \leq \phi(t), \tag{5.3}$$

$$\left|{}_0^{LC}D_t^{\mathfrak{z}}\Lambda(t) - \varphi(t, \Lambda(t))\right| \leq \epsilon\phi(t). \tag{5.4}$$

Definition 5.1. *The IVP* (5.1) *reveals Ulam–Hyers (U-H) stability if* $\exists\ k_j > 0$ *such that* $\forall\ \epsilon > 0$, *and for each* $\Lambda \in \mathbb{C}[0, +\infty)$ *satisfying* (5.2), *a solution* $\Re \in \mathbb{C}[0, +\infty)$ *of* (5.1) *is present, satisfying* $|\Lambda(t) - \Re(t)| \leq \epsilon k_j$.

Definition 5.2. *The IVP* (5.1) *exhibits generalized Ulam–Hyers (G-U-H) stability if* $\exists\ k_j \in \mathbb{R}^+$ *exists such that* $k_j(0) = 0$, $\forall\ \epsilon > 0$, *and* $\Lambda \in \mathbb{C}$ *of Eq* (5.3). *There exists a solution* $\Re \in \mathbb{C}$ *of* (5.1) *fulfilling* $|\Lambda(t) - \Re(t)| \leq k_j(\epsilon)$.

Definition 5.3. *The IVP* (5.1) *demonstrates Ulam–Hyers-Rassias (U-H-R) stability if* $\exists\ k_{j,l} \in \mathbb{R}$, $\forall\ \epsilon > 0$, *and for every* $\Lambda \in \mathbb{C}$ *of* (5.4), *there exists a solution* $\Re \in \mathbb{C}$ *of* (5.1) *addressing* $|\Lambda(t) - \Re(t)| \leq \epsilon k_{j,l}\phi(t)$.

Definition 5.4. *The IVP* (5.1) *has generalized Ulam–Hyers–Rassias (G-U-H-R) stability if* $\exists\ k_{j,l} \in \mathbb{R}$ *and for every* $\Lambda \in \mathbb{C}$ *of* (5.3), *there exists a solution* $\Re \in \mathbb{C}$ *of* (5.1) *with* $|\Lambda(t) - \Re(t)| \leq k_{j,l}\phi(t)$, *with respect to* ϕ.

Hypothesis 1. *Let* $\phi \in \mathbb{C}[0, \infty)$ *be an accumulating function, then* $\exists\ \varepsilon_\varphi > 0$, *implying that*

$$\frac{1}{\Gamma(\mathfrak{z})}\int_0^t (t-\Re)^{\mathfrak{z}-1}\phi(\Re)\, d\Re \leq \varepsilon_\varphi\phi(t), \qquad (t \geq 0).$$

Lemma 5.2. *Consider* F_1 *and* F_2 *as continuous functions defined over* $[0, \infty) \times [0, \infty)$. *If* F_2 *is increasing and* $\exists\ \mu, \zeta > 0$, *this implies*

$$F_1(t) \leq F_2(t) + \mu\int_0^t (t-\Re)^{\zeta-1} F_1(\Re)\, d\Re, \qquad (t \geq 0).$$

Then,

$$F_1(t) \leq F_2(t) + \int_0^t \left[\sum_{j=0}^{\infty} \frac{(\mu\Gamma(\zeta))^j}{\Gamma(j\zeta)}(t-\Re)^{\zeta-1} F_2(\Re)\right] d\Re.$$

If $F_2(t) = a$ *(constant), then* $F_1(t) \leq a\mathrm{E}_\zeta\left(\mu\Gamma(\zeta)\, t^{\zeta}\right)$, *where* $\mathrm{E}_\zeta(\bullet)$ *is the Mittag–Leffler function.*

Theorem 5.3. *If the criteria of Hypothesis 1 is fulfilled, then the IVP* (5.1) *is G-U-H-R stable.*

Proof. Assuming Λ is a solution of (5.3) over the interval $\mathbb{C}[0, \mathsf{T})$, we consider $\Re$ as a solution of (5.1). Thus,

$$\begin{aligned}
&\left|\Lambda(t) - \Lambda_0(t) - \frac{1}{\Gamma(\mathfrak{z})}\int_0^t (t-\Re)^{\mathfrak{z}-1}\varphi(\Re, \Lambda(\Re))d\Re\right| \\
\leq &\frac{1}{\Gamma(\mathfrak{z})}\int_0^t (t-\Re)^{\mathfrak{z}-1}\varphi(\Re)\, d\Re \\
\leq &\chi_\varphi\varphi(t).
\end{aligned}$$

It follows from these connections that

$$|\Lambda(t) - \Re(t)| \leq \chi_\varphi\varphi(t) + \frac{N}{\Gamma(\mathfrak{z})}\int_0^t (t-\Re)^{\mathfrak{z}-1}\,|\Lambda(\Re) - \Re(\Re)|\, d\Re.$$

As per *Lemma* 5.2, there exists a constant $N^* > 0$ that is independent of $\chi_\varphi \varphi(t)$. This constant satisfies $|\Lambda(t) - \Re(t)| \leq N^* \chi_\varphi \varphi(t)$, denoted as $a_{f,\varphi}\varphi(t)$. As a result, the IVP (5.1) can be classified as having G-U-H-R stability. □

Corollary 5.3.1. *Using the same logic as in Theorem 5.3, one can demonstrate that IVP* (5.1)*, coupled by* (5.2)*, achieves U-H-R stability.*

Corollary 5.3.2. *By employing the same techniques of Theorem 5.3 with inequality* (5.4)*, one can demonstrate IVP* (5.1) *is U–H stable.*

6. Numerical algorithm

We provide a numerical approach for our suggested model (3.1) in this section. The numerical simulations were performed using Google Colab, a cloud-based computing platform that offers access to Python runtime environments with standard CPU and GPU resources.

First, we provide the predictor-corrector technique [34] for solving FDE with starting conditions:

$$ {}_0^{LC}D_t^{\mathfrak{z}}\Lambda(t) = \varphi(t, \Lambda(t)), \mathfrak{z} > 0, \tag{6.1}$$

and initial conditions

$$\Lambda^k(0) = \Lambda_0^k, \tag{6.2}$$

where $k = 0, 1, 2, 3, ..., \lceil \mathfrak{z} \rceil - 1$.

If we take the integral of (6.1) according to (2.1), it gives us a second order Volterra integral equation:

$$\Lambda(t) = \sum_{q=0}^{\lceil \mathfrak{z} \rceil - 1} \Lambda^q(0)\frac{t^q}{q!} + \frac{1}{\Gamma(\mathfrak{z})}\int_0^t (t-s)^{\mathfrak{z}-1} f(s, \Lambda(s))ds. \tag{6.3}$$

Now, set $h = \frac{\mathrm{T}}{N}$ and $t_m = mh, (m = 0, 1, 2, ..., N)$.

As a result, the Eq (6.3) may be discretized in the following way:

$$\Lambda_{i+1} = \sum_{q=0}^{\lceil \mathfrak{z} \rceil - 1} \Lambda^q(0)\frac{t_{i+1}^q}{q!} + \frac{h^{\mathfrak{z}}}{\Gamma(\mathfrak{z}+2)}\left\{ f\left(t_{i+1}, \Lambda_{i+1}^p\right) + \sum_{q=0}^{i} a_{i+1,q} f\left(t_q, \Lambda_q\right)\right\}, \tag{6.4}$$

where,

$$a_{q,m+1} = \begin{cases} m^{\mathfrak{z}+1} - (m-\mathfrak{z})(m+1)^{\mathfrak{z}}, & q = 0, \\ (m-q+2)^{\mathfrak{z}+1} + (m-q)^{\mathfrak{z}+1} - 2(m-q+1)^{\mathfrak{z}+1}, & 1 \leq q \leq m, \\ 1, & q = m+1, \end{cases} \tag{6.5}$$

and Λ_{i+1}^p is given by

$$\Lambda_{i+1}^p = \sum_{q=0}^{\lceil \mathfrak{z} \rceil - 1} \Lambda^q(0)\frac{t_{i+1}^q}{q!} + \frac{1}{\Gamma(\mathfrak{z})}\left\{ \sum_{q=0}^{i} b_{i+1,q} f\left(t_q, \Lambda_q\right)\right\}. \tag{6.6}$$

and

$$b_{q,m+1} = \frac{h^{\mathfrak{z}}}{\mathfrak{z}}\left((m+1-q)^{\mathfrak{z}} - (m-q)^{\mathfrak{z}}\right); 0 \leq q \leq m. \tag{6.7}$$

The stability and convergence of this method are mentioned in [35].

We utilize the above proposed numerical scheme on model (3.1) as:

$$\begin{aligned} H_{n+1} =& H(0) + \frac{h^{\mathfrak{z}}}{\Gamma(\mathfrak{z}+2)}\left\{ J_1(t_{n+1}, H_{n+1}^p, D_{n+1}^p, A_{n+1}^p) \right. \\ &\left. + \sum_{q=0}^{n} a_{q,n+1} J_1(t_q, H_q, D_q, A_q)\right\}. \end{aligned} \tag{6.8}$$

$$\begin{aligned} D_{n+1} =& D(0) + \frac{h^{\mathfrak{z}}}{\Gamma(\mathfrak{z}+2)}\left\{ J_2(t_{n+1}, H_{n+1}^p, D_{n+1}^p, A_{n+1}^p) \right. \\ &\left. + \sum_{q=0}^{n} a_{q,n+1} J_2(t_q, H_q, D_q, A_q)\right\}. \end{aligned} \tag{6.9}$$

$$\begin{aligned} A_{n+1} =& A(0) + \frac{h^{\mathfrak{z}}}{\Gamma(\mathfrak{z}+2)}\left\{ J_3(t_{n+1}, H_{n+1}^p, D_{n+1}^p, A_{n+1}^p) \right. \\ &\left. + \sum_{q=0}^{n} a_{q,n+1} J_3(t_q, H_q, D_q, A_q)\right\}, \end{aligned} \tag{6.10}$$

where,

$$H_{n+1}^p = S(0) + \frac{1}{\Gamma(\mathfrak{z})}\sum_{q=0}^{n} b_{q,n+1} J_1(t_q, H_q, D_q, A_q). \tag{6.11}$$

$$D_{n+1}^p = T(0) + \frac{1}{\Gamma(\mathfrak{z})}\sum_{q=0}^{n} b_{q,n+1} J_2(t_q, H_q, D_q, A_q). \tag{6.12}$$

$$A_{n+1}^p = V(0) + \frac{1}{\Gamma(\mathfrak{z})}\sum_{q=0}^{n} b_{q,n+1} J_3(t_q, H_q, D_q, A_q). \tag{6.13}$$

7. Numerical simulation and discussion

In this section, we perform a series of numerical simulations to demonstrate the dynamic behavior of a breast cancer model under both fractional and integer order frameworks. These simulations offer empirical support for the theoretical results developed and emphasize the biological significance of fractional models in capturing realistic cancer dynamics. The numerical simulations which are generated using scheme (6.8)–(6.10) and (6.11)–(6.13) are designed to show the behaviours for $\mathfrak{z} = 0.7, 0.8, 0.9, 1$.

We first investigate the impact of varying fractional orders $\mathfrak{z} = 0.7, 0.8, 0.9, 1$ on the populations of healthy and cancerous cells. With initial conditions set to $H(0) = 1460$ (healthy cells) and $D(0) = 0.01$ (initial cancer cells). Over a 40-day span, Figures 1 and 2 reveal that fractional orders below $\mathfrak{z} = 1$ induce a more gradual decline in healthy cells and a slower increase in dead cancer cells. This behavior is biologically significant as it mirrors the progressive, gradual nature of cancer spread and the immune system's slower response in early stages of disease progression. The fractional model's ability to capture these nuanced dynamics offers a more realistic representation of tumor growth over time, compared to the immediate responses often seen in integer-order models.

When incorporating treatment factors—such as chemotherapy, ketogenic diet, and monoclonal antibody therapies—the simulations with updated initial conditions $H(0) = 500$, $D(0) = 100$, and $M(0) = 90$ (therapy agents) reveal an increase in the healthy cell population (Figure 3) and a decrease in cancer cells (Figure 4). The fractional orders further illustrate how these control measures maintain their effect over time, as lower $\mathfrak{z}$ values produce a more prolonged response to therapy. This prolonged efficacy is critical biologically, as it reflects how fractional models can simulate the long-term benefits of therapies more accurately, capturing the slow and continuous recovery of healthy cells under treatment.

Figures 5 and 6 illustrate that the therapeutic impact of control parameters remains effective up to $D(0) = 179$. However, beyond this threshold, the effectiveness of the treatments gradually decreases, as indicated in Figures 7 and 8. In comparison, the classical integer-order model exhibits a faster decrease in therapeutic impact, with effectiveness persisting only up to $D(0) = 131$. This difference highlights the biological significance of fractional models, which can represent the gradual but prolonged influence of treatments even in advanced stages of cancer.

To address the observed decline in effectiveness beyond $D(0) = 179$, we introduce the z control into the model (as shown in Eq (3.1)). Figures 9 and 10 reveal that the inclusion of this additional regulatory mechanism helps to maintain healthy cell levels and continues to suppress cancer cells, effectively extending the therapeutic impact.

The comparison between Figures 7 and 8 (without z-control) and Figures 9 and 10 (with z-control) further emphasizes the value of z-control. It shows that the additional control provides continued therapeutic effectiveness even when $D(0) > 179$, providing insight into the flexibility of the fractional model for adaptive and prolonged treatment strategies. This adaptability underscores the advantage of the fractional model in addressing complex, advanced-stage cancer dynamics where traditional models may fall short.

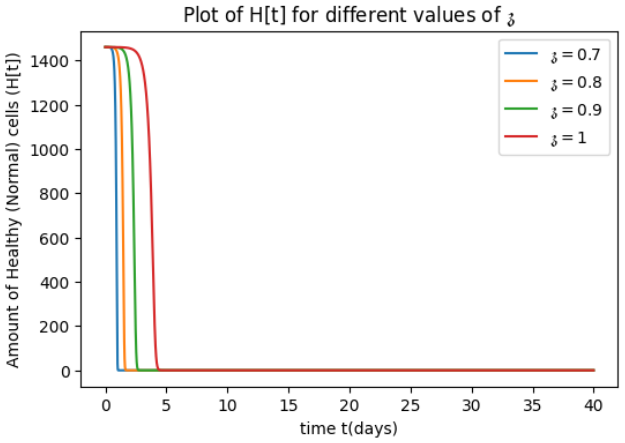

Figure 1. Decay of healthy cells without treatment.

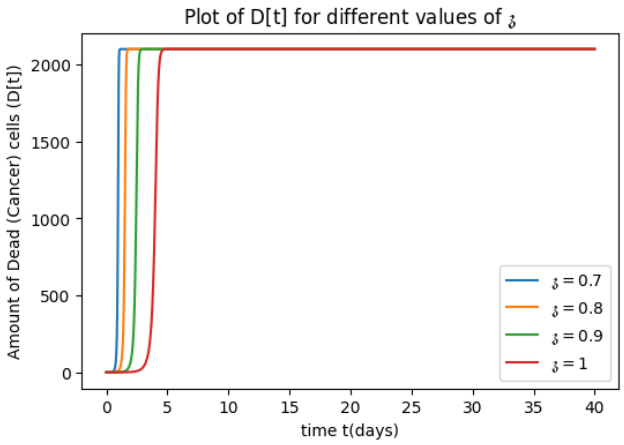

Figure 2. Growth of dead cells without treatment.

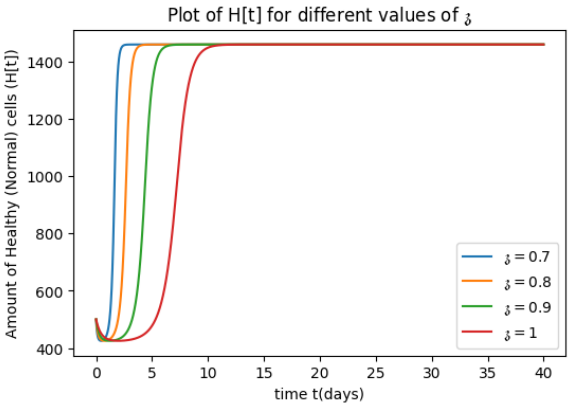

Figure 5. Growth of healthy cells with treatment at D(0) = 179.

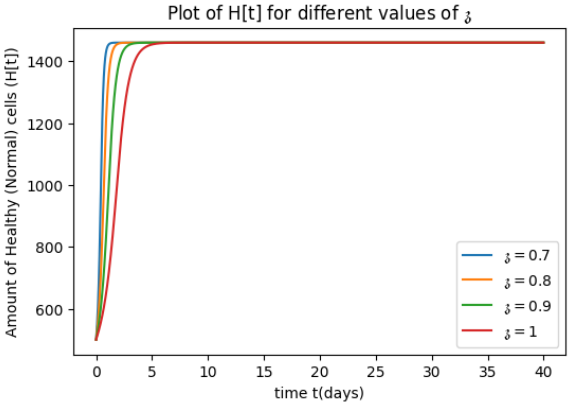

Figure 3. Growth of healthy cells with treatment at D(0) = 100.

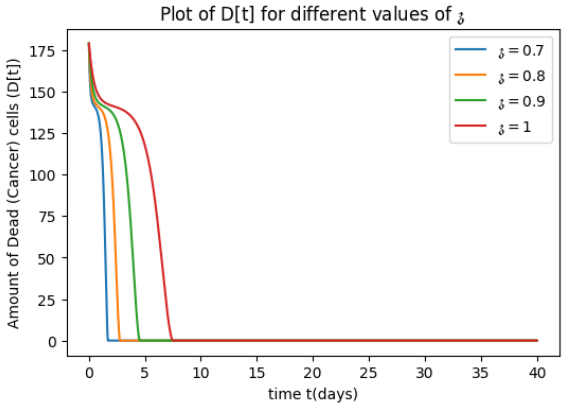

Figure 6. Decay of dead cells with treatment at D(0) = 179.

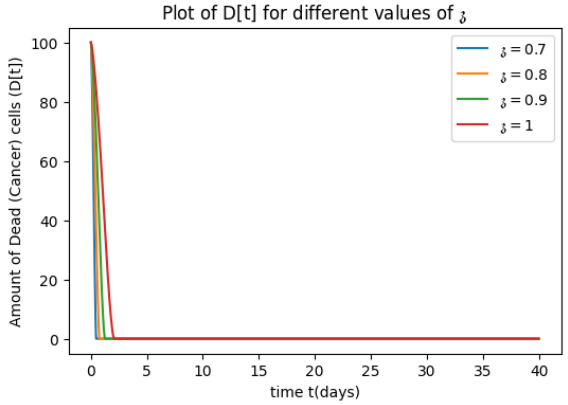

Figure 4. Decay of dead cells with treatment at D(0) = 100.

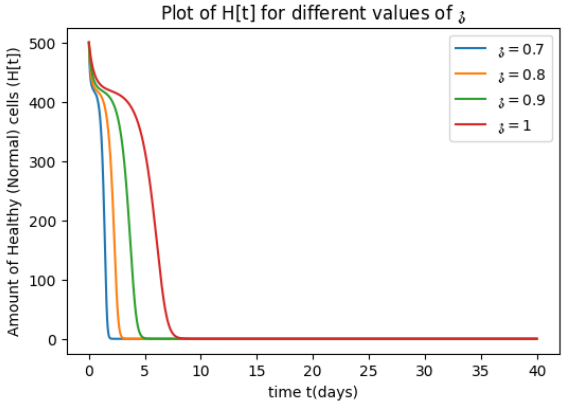

Figure 7. Decay of healthy cells with treatment and without z–control.

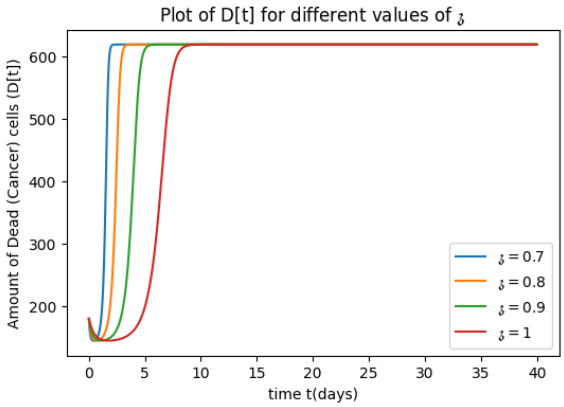

Figure 8. Growth of dead cells with treatment and without z–control.

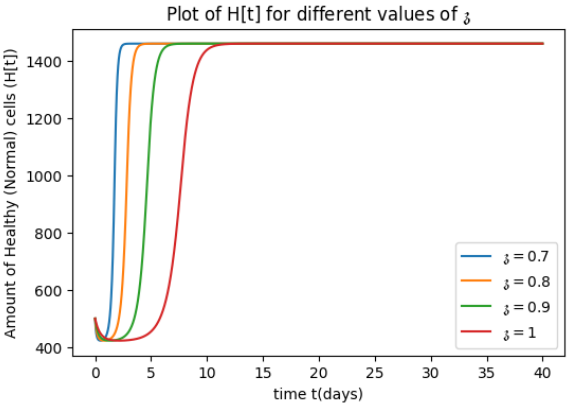

Figure 9. Growth of healthy cells with treatment and z–control.

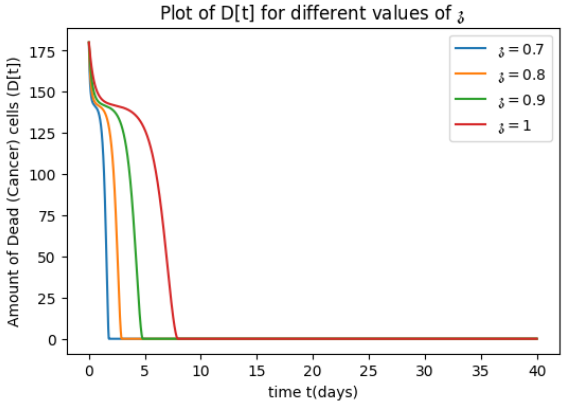

Figure 10. Decay of dead cells with treatment and z–control.

8. Conclusions

In this work, we developed a comprehensive fractional-order mathematical model to study the dynamics of breast cancer growth and its control using chemotherapy. The model incorporates three crucial therapeutic control parameters-monoclonal antibody drugs, a ketogenic diet, and a z-control strategy-each reflecting different clinical interventions aimed at reducing tumor burden and enhancing patient outcomes.

To ensure the mathematical rigor of the proposed model, we established the existence and uniqueness of the solutions by applying Sadovskii's fixed-point theorem, which confirms the robustness and reliability of the model under the framework of fractional differential equations. Furthermore, we analyzed the global stability of the system using the Hyers–Ulam stability criteria, which demonstrated that the model consistently responds to small perturbations and remains stable over time, thereby reinforcing the model's capacity to simulate real-world biological dynamics accurately.

We performed numerical simulations using a predictor-corrector method, which illustrated the significant advantages of the fractional-order approach in capturing the complex dynamics of breast cancer progression. Compared to classical integer-order models, the fractional model exhibited improved flexibility, memory effects, and long-term prediction capabilities, which are essential features when dealing with biological systems.

The findings from this study provide a strong theoretical foundation for developing advanced breast cancer treatment strategies that are not only mathematically sound but also clinically relevant. The inclusion of control parameters related to immunotherapy, metabolic interventions, and experimental variables further enhances the model's applicability in real-world therapeutic design.

This research can be extended by integrating alternative fractional derivative operators such as the Atangana–Baleanu or Caputo–Fabrizio operators, which may offer additional modeling flexibility and biological interpretability. Moreover, applying this model to real clinical or patient-specific data could provide more accurate insights into tumor dynamics, optimize treatment regimens,

and potentially support personalized medicine approaches in breast cancer care.

Use of Generative-AI tools declaration

The authors declare they have not used Artificial Intelligence (AI) tools in the creation of this article.

Conflict of interest

All authors confirm that they have no competing interests related to this article.

References

1. C. W. Evans, The invasion and metastatic behaviour of malignant cells, In: *The metastatic cell: behavior and biochemistry*, Chapman and Hall: London, UK, 1991, 137–214.
2. M. Patel, S. Nagl, *The role of model integration in complex systems modelling: an example from cancer biology*, Springer Berlin, Heidelberg, 2010. https://doi.org/10.1007/978-3-642-15603-8
3. D. A. Botesteanu, S. Lipkowitz, J. M. Lee, D. Levy, Mathematical models of breast and ovarian cancers, *WIREs Syst. Biol. Med.*, **8** (2016), 337–362. https://doi.org/10.1002/wsbm.1343
4. S. K. Dey, S. Charlie Dey, Mathematical modeling of breast cancer treatment, In: S. Sarkar, U. Basu, S. De, *Applied mathematics*, Springer Proceedings in Mathematics & Statistics, New Delhi: Springer, **146** (2015), 149–160. https://doi.org/10.1007/978-81-322-2547-8_13
5. S. I. Oke, M. B. Matadi, S. S. Xulu, Optimal control analysis of a mathematical model for breast cancer, *Math. Comput. Appl.*, **23** (2018), 21. https://doi.org/10.3390/mca23020021
6. P. Shah, T. Shah, Adaptive neuro fuzzy inference system based classifier in diagnosis of breast cancer, *Results Control Optim.*, **14** (2024), 100358. https://doi.org/10.1016/j.rico.2023.100358
7. P. J. Shah, T. P. Shah, The ultimate kernel machine for diagnosis of breast cancer, *Int. J. Appl. Pattern Recognit.*, **7** (2022), 1–14. https://doi.org/10.1504/IJAPR.2022.122259
8. P. Shah, T. Shah, Identification of breast tumor using hybrid approach of independent component analysis and deep neural network, *Int. J. Intell. Syst. Appl. Eng.*, **9** (2021), 209–219.
9. P. J. Shah, T. P. Shah, Regularized deep neural network in identification of breast cancer, *Solid State Technol.*, **63** (2020), 22704–22715.
10. H. C. Wei, Mathematical modeling of ER-positive breast cancer treatment with AZD9496 and palbociclib, *AIMS Math.*, **5** (2020), 3446–3455. https://doi.org/10.3934/math.2020223
11. I. Podlubny, Fractional differential equations: an introduction to fractional derivatives, fractional differential equations, to methods of their solution and some of their applications, In: *Mathematics in science and engineering*, San Diego: Academic Press, **198** (1998).
12. T. Q. Tang, Z. Shah, E. Bonyah, R. Jan, M. Shutaywi, N. Alreshidi, Modeling and analysis of breast cancer with adverse reactions of chemotherapy treatment through fractional derivative, *Comput. Math. Methods Med.*, **2022** (2022), 5636844. https://doi.org/10.1155/2022/5636844
13. E. Ucar, N. Özdemir, E. Altun, Fractional order model of immune cells influenced by cancer cells, *Math. Model. Nat. Phenom.*, **14** (2019), 1–12. https://doi.org/10.1051/mmnp/2019002
14. W. Adel, H. M. Srivastava, M. Izadi, A. Elsonbaty, A. El-Mesady, Dynamics and numerical analysis of a fractional-order toxoplasmosis model incorporating human and cat populations, *Bound. Value Probl.*, **2024** (2024), 152. https://doi.org/10.1186/s13661-024-01965-w
15. C. Baishya, S. J. Achar, P. Veeresha, An application of the Caputo fractional domain in the analysis of a COVID-19 mathematical model, *Contemp. Math.*, **5** (2024), 255–283. https://doi.org/10.37256/cm.5120242363

16. C. Baishya, M. K. Naik, R. N. Premakumari, Design and implementation of a sliding mode controller and adaptive sliding mode controller for a novel fractional chaotic class of equations, *Results Control Optim.*, **14** (2024), 100338. https://doi.org/10.1016/j.rico.2023.100338

17. M. Izadi, H. M. Srivastava, Robust QLM-SCFTK matrix approach applied to a biological population model of fractional order considering the carrying capacity, *Discrete Contin. Dyn. Syst. Ser. S*, **18** (2025), 1159–1181. https://doi.org/10.3934/dcdss.2023101

18. M. K. Naik, C. Baishya, R. N. Premakumari, M. E. Samei, Navigating climate complexity and its control via hyperchaotic dynamics in a 4D Caputo fractional model, *Sci. Rep.*, **14** (2024), 18015. https://doi.org/10.1038/s41598-024-68769-x

19. M. K. Naik, C. Baishya, R. N. Premakumari, P. Veeresha, Exploring ocean pH dynamics via a mathematical modeling with the Caputo fractional derivative, *J. Umm Al-Qura Univ. Appl. Sci.*, **11** (2025), 421–437. https://doi.org/10.1007/s43994-024-00168-4

20. R. N. Premakumari, C. Baishya, S. Rezapour, M. K. Naik, Z. M. Yaseem, S. Etemad, Qualitative properties and optimal control strategy on a novel fractional three-species food chain model, *Qual. Theory Dyn. Syst.*, **23** (2024), 252. https://doi.org/10.1007/s12346-024-01110-z

21. A. Singh, A. Chavada, N. Pathak, Fractional calculus approach to Pancreatic cancer therapy: modeling tumor and immune interactions with siRNA treatment, *Int. J. Appl. Comput. Math*, **11** (2025), 61. https://doi.org/10.1007/s40819-025-01873-2

22. A. Chavada, N. Pathak, A note on Lyapunov-type inequalities for fractional boundary value problems with Sturm-Liouville boundary conditions, *J. Math. Ext.*, **15** (2021), 1–12. https://doi.org/10.30495/JME.2021.1634

23. N. Pathak, A. Chavada, M. Thakkar, Qualitative analysis of Caputo fractional mathematical model of Pancreatic Cancer, *Math. Applicanda*, **52** (2024), 205-226. https://doi.org/10.14708/ma.v52i2.7272

24. S. J. Achar, C. Baishya, P. Veeresha, L. Akinyemi, Dynamics of fractional model of biological pest control in tea plants with Beddington–DeAngelis functional response, *Fractal Fract.*, **6** (2021), 1. https://doi.org/10.3390/fractalfract6010001

25. E. Ilhan, P. Veeresha, H. M. Baskonus, Fractional approach for a mathematical model of atmospheric dynamics of CO_2 gas with an efficient method, *Chaos, Soliton. Fract.*, **152** (2021), 111347. https://doi.org/10.1016/j.chaos.2021.111347

26. P. Veeresha, The efficient fractional order based approach to analyze chemical reaction associated with pattern formation, *Chaos, Soliton. Fract.*, **165** (2022), 112862. https://doi.org/10.1016/j.chaos.2022.112862

27. P. Veeresha, E. Ilhan, D. G. Prakasha, H. M. Baskonus, W. Gao,, A new numerical investigation of fractional order susceptible-infected-recovered epidemic model of childhood disease, *Alex. Eng. J.*, **61** (2022), 1747–1756. https://doi.org/10.1016/j.aej.2021.07.015

28. P. Veeresha, D. G. Prakasha, D. Baleanu, Analysis of fractional Swift-Hohenberg equation using a novel computational technique, *Math. Methods Appl. Sci.*, **43** (2020), 1970–1987. https://doi.org/10.1002/mma.6022

29. J. E. Solís-Pérez, J. F. Gómez-Aguilar, A. Atangana, A fractional mathematical model of breast cancer competition model, *Chaos, Soliton. Fract.*, **127** (2019), 38–54. https://doi.org/10.1016/j.chaos.2019.06.027

30. A. Yousef, F. Bozkurt, T. Abdeljawad, Mathematical modeling of the immune-chemotherapeutic treatment of breast cancer under some control parameters, *Adv. Differ. Equ.*, **2020** (2020), 696. https://doi.org/10.1186/s13662-020-03151-5

31. D. K. Dave, T. P. Shah, Stability analysis and Z-control of breast cancer dynamics, *Adv. Appl. Math. Sci.*, **21** (2021), 343–363.

32. H. M. Srivastava, M. Izadi, Generalized shifted airfoil polynomials of the second kind to solve a class of singular electrohydrodynamic fluid model of fractional order, *Fractal Fract.*, **7** (2023), 94. https://doi.org/10.3390/fractalfract7010094

33. L. Mahto, S. Abbas, Existence and uniqueness of solution of Caputo fractional differential equations, *AIP Conf. Proc.*, **1479** (2012), 896–899. https://doi.org/10.1063/1.4756286

34. K. Diethelm, N. J. Ford, A. D. Freed, A predictor-corrector approach for the numerical solution of fractional differential equations, *Nonlinear Dyn.*, **29** (2002), 3–22. https://doi.org/10.1023/A:1016592219341

35. K. Diethelm, N. J. Ford, A. D. Freed, Detailed error analysis for a fractional Adams method, *Numer. Algorithms*, **36** (2004), 31–52. https://doi.org/10.1023/B:NUMA.0000027736.85078.be

AIMS Press